

## PHOTOABSORPTION OF X-RAYS IN THE MAGNETIC COMPACT STAR

Yonggi Kim

Yonsei University Observatory, Seoul 120-749, Korea

*(Received November 25, 1992; Accepted December 19, 1992)*

### ABSTRACT

Radiation due to accretion from an accretion disc around the intermediate polars and photoabsorption of this radiation in the accretion funnel have been taken into account as a phenomenological model to study the physics of the magnetic funnel in the magnetic compact star. The first results show that such a model scenario can be used to estimate some parameters in these systems. Some constraints of this model regarding to the observational data of one intermediate polar, EX Hya, are also discussed.

### 1. INTRODUCTION

An accretion disc can be formed around a magnetic compact star in a close binary system if its magnetic field is not strong enough (intermediate polar, IP). The matter in the disc is assumed to circulate around the compact star at the Keplerian velocity. The rotational axis of the intermediate polars is not aligned with the magnetic axis. In this case the accretion flow is funneled at some radius where the ram pressure is governed by the magnetic pressure. Within this radius the plasma flows toward the magnetic poles of the compact star along the magnetic field lines and accretes onto a small arc-shaped region on the stellar surface. The intersection angle of the magnetic field with the disc and the component of the gravitational vector parallel to the field lines change around the disc. Therefore, the accretion rate toward the upper and lower pole varies as a function of the azimuthal angle of the disc. It is expected that the largest fraction of matter accretes from the side of the disc closest to the magnetic pole. Near the stellar surface the infalling matter produces a shock which gives rise to X-ray emission modulated with the rotational period. A new phenomenological approach to the distribution of accretion rate as a function of the rotational phase is presented in this paper.

Photoabsorption by the material in the accretion funnel is mainly responsible for the X-ray modulation with the rotational phase. A recent review of this spin modulated X-ray emission is given by Norton and Watson (1989) with regard to the observational analysis of the intermediate polars. From the spectral fits of the observational datasets they derived the

absorption column density of the hard X-ray emitting region. We show that the observed column density,  $N_{HI}$ , does not come from the hard X-ray emitting region, but from the matter in the accretion funnel.

In contrast to their approach we begin with some physical model parameters of the system, which are inferred in the observation until now. Using conservation laws we then try to estimate the analytic absorption column density along the line of sight at a given rotational phase. Finally, we compute the X-ray spectrum and light curves. Energy dependence of the X-ray modulation has been mainly inspected because it can be easily predicted from the energy dependence of photoabsorption. The eclipsing cataclysmic variable EX Hya, one of the intermediate polars, has been taken into account in this model because the physical parameters of EX Hya are well studied until now in X-ray and optical light. We will use a phenomenological model to derive the more reasonable parameters being consistent with observations (Beuermann and Osborne 1985, Rosen *et al.* 1988). In the following we present *first results of our phenomenological model of the accretion funnel.*

## 2. MODEL SCENARIO

It is usually adapted that the dipole geometry describes the magnetic accretion geometry of the compact star. The dipole geometry can be written in a spherical coordinate  $(r, \theta, \phi)$  at the given value of  $\phi$  as following,

$$r = R_m \sin^2 \theta, \quad (1)$$

where  $R_m$  is the radial distance of the magnetic field line at  $\phi = 90^\circ$ .

The fact that the magnetic axis is inclined to the disc ( $\beta$ ) may lead to an asymmetry in the accretion pattern on to the magnetic compact star. Figure 1 shows a dipole geometry used here. In order to explain the motion of matter due to this asymmetry we introduce two functions; the distribution function of the accretion rate around the interaction ring ( $f_1$ ) and the fraction function giving the fraction of the matter accreted toward the upper pole ( $f_2$ ). The former is dependent on the magnetic pressure,

$$\begin{aligned} f_1 &\sim \frac{|B|^2}{8\pi} \\ &= \left( \mu \frac{\sqrt{1 + 3 \cos^2 \theta_1}}{r^3} \right)^2, \end{aligned} \quad (2)$$

where  $\theta_1$  can be written from the dipole geometry (Eq. 1) as

$$\sin \theta_1(\gamma) = \sqrt{\frac{R_w d}{r} (1 - \sin^2 \beta \cos \gamma)}. \quad (3)$$

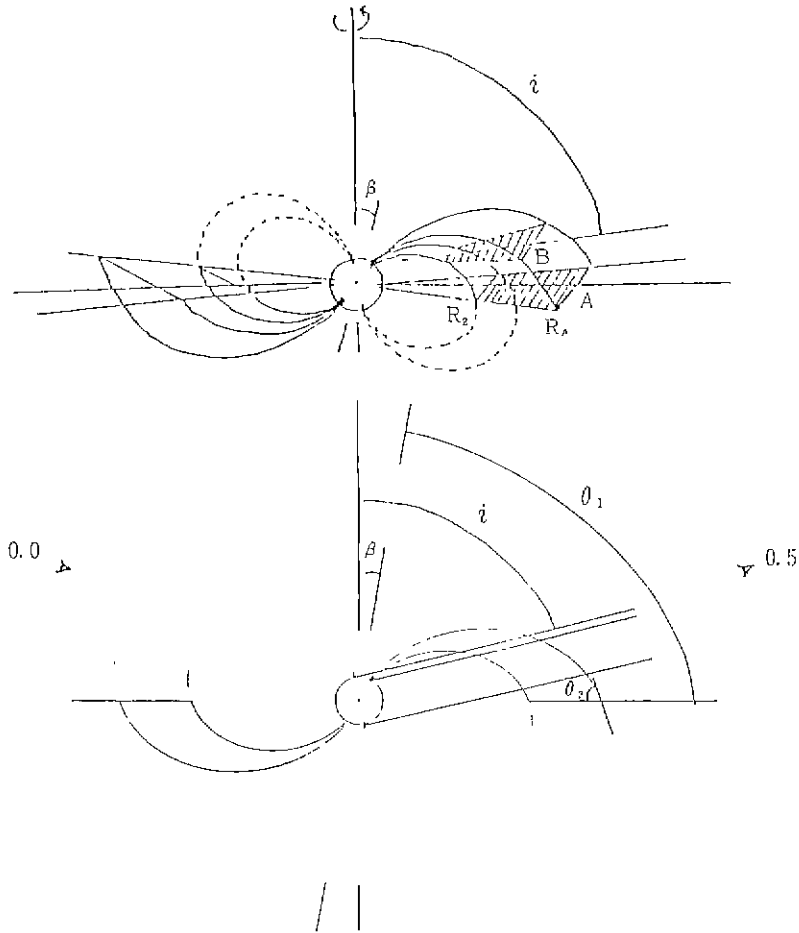


Figure 1. Geometry of the accretion funnel. a) schematic geometry of the dipole magnetic field and b) side-on view of the magnetic field geometry.

Here  $\theta_1$  and  $\gamma$  represent, the angle from the magnetic axis and the azimuthal angle at A in Figure 1b, respectively. The parameters  $\mu$  and  $R_{wd}$  are the magnetic moment and the radius of the magnetic compact star. Since  $r$  and  $\mu$  are constant along the interaction ring,  $f_1$  can be described by  $\theta_1$  only. We introduce therefore a distribution function

$$f_1 = (1 + 3 \cos^2 \theta_1)^a, \quad (4)$$

where  $a$  is a free parameter.

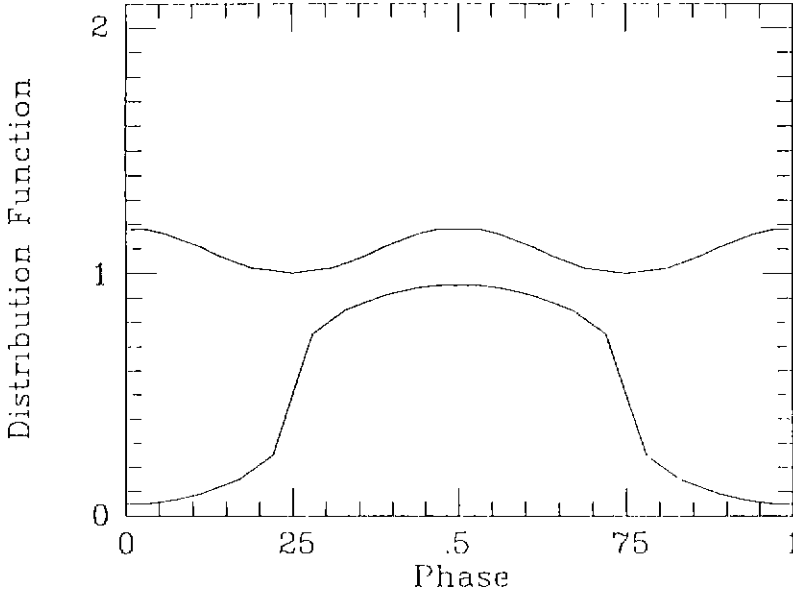


Figure 2. Adapted distribution function. a)  $f_1 = (1 + 3 \cos^2 \theta_1)$  (upper curve)  
 b)  $f_2 = (\frac{90 - \theta_2}{90})^{0.5} + 0.5$  (lower curve).

The latter function must be introduced because the matter will accrete preferentially from the side of the disc that is closest to the magnetic pole (main accretion indicated by solid field line and sub accretion indicated by pointed field line in Figure 1b). This function may be connected with the variation of the component of the gravitational vector parallel to the field line around the disc. For an oblique rotator this component is a function of the intersection angle of the magnetic field with the disc ( $\theta_2$  in Figure 1b). At rotational phases 0.25 and 0.75, half of the matter will accrete toward each of the poles. The fraction of the upper accretion stream must be lowest at phase 0.0 and highest at phase 0.5. We choose this function as

$$f_2 = (\frac{90 - \theta_2}{90})^b + 0.5, \quad (5)$$

where the exponent  $b$  is another free parameter. The fraction of the accretion toward the lower pole is  $1 - f_2$ . In Figure 2 one can see the adapted distribution functions,  $f_1$  and  $f_2$ .

Still unclear is with which velocity ( $v_1$ ) the matter begins to accrete. Since the matter circulates around the disc with the Keplerian velocity ( $v_{Kep}$ ) it is sure that  $v_1$  is a fraction of  $v_{Kep}$ . Our calculations with varying  $a$ ,  $b$  and  $v_1$  have shown that the modulation of high

energy X-rays is not very sensitive to these free parameters. For the purpose of this study we therefore take  $a = 3$ ,  $b = 0.5$  and  $v_1 = v_{Kep}$ .

Hard X-rays characterized by the shock temperature  $T_s = 10$  K (10 keV) are formed just above the stellar surface by the infalling accreted matter. Half of the accretion luminosity will be directed toward the stellar surface. A part of this radiation is reflected directly, while the rest is absorbed at the surface and is re-radiated as black body emission (soft X-rays). We adapted in this paper that a thermal Bremsstrahlung amounts to 0.7 of the total accretion luminosity. The soft X-ray component has no contribution to the observed spectrum because it may be fully absorbed by the accretion funnel and interstellar medium ( $N_{ISM} = 10^{21} \text{ cm}^{-2}$ ).

We have divided the X-ray emitting region into 36 point sources around the upper pole and another 36 sources around the lower pole. The luminosity of these point sources is dependent on the accretion rate varying with the phase as seen in Figure 2. At every phase the visibility of these 72 point sources has been checked. The radiation from the visible point sources at a given phase is weakened by the cool matter in the accretion funnel. There are three ways to pass the accretion funnel for any light beam (Fig. 1b). The sources behind the rotational axis experience more column density than these in front of the rotational axis. The point sources below the accretion disc suffer another column density.

The density at any point  $(r, \theta)$  (area B in Figure 1a) can be easily estimated from the usual conservation (energy, mass and magnetic flux)

$$\rho = \frac{\rho_1 v_1}{v} \left( \frac{R_1}{r} \right)^3 \left( \frac{1 + 3\cos^2\theta}{1 + 3\cos^2\theta_1} \right)^{0.5} \quad (6)$$

where  $r$  is the radial distance,  $\theta$  the angle from the magnetic axis, and  $v$  the velocity of matter at this point, and  $R_1, \theta_1$ , and  $v_1$  are the radial distance, the angle from the magnetic axis, and velocity for the runaway of matter in the magnetic field at the interaction zone.

Combining the density with the length of the accretion funnel along the line of sight results in the column density. The length of the accretion funnel at B can be estimated from the dipole geometry (Eq. 1). With a simple analytic function from Morrison and McCammon (1983) the X-ray absorption cross section ( $\sigma$ ) per H-atom of a cosmic plasma is calculated in order to guess the optical depth ( $\tau = \sigma N_{HI}$ ). The photoabsorption of the hard X-ray emission can now be calculated. It has to be noted that we use the column density in the accretion funnel absorbing the hard X-ray, not the column density of the hard X-ray emission region as done by Norton and Watson (1989). Net photoelectric cross section per H-atom used here is shown in Figure 3.

Due to the inhomogeneities in the accretion funnel the matter is not well described by a simple absorber rather than by a partially filled volume, *i.e.* some fraction of radiation (filling factor) is absorbed, while another fraction passes the funnel unabsorbed. This idea has been justified by Rosen *et al.* (1988), Norton and Watson (1989) and King and Lasota (1990). Our calculation has been carried out for all phases starting with the parameters of EX Hya derived by Hellier *et al.* (1987) and Rosen *et al.* (1988).

We have then tried to improve the parameters using our phenomenological model. The following results have been calculated using our final parameters (Table 1). In Figure 4 and Figure 5 only one parameter is varied whilst the other parameters are kept unchanged.

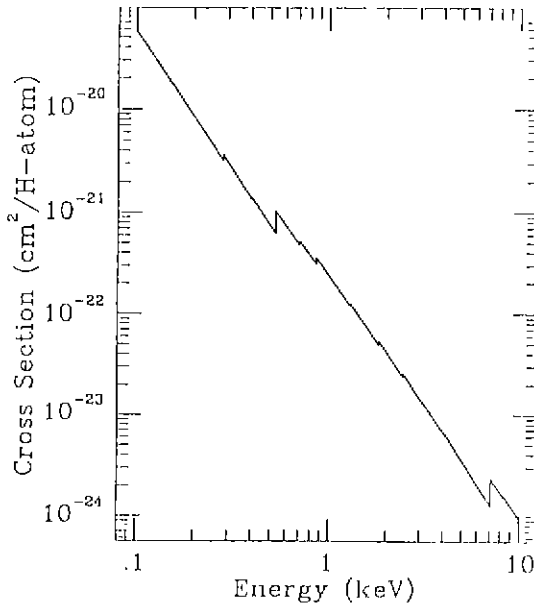


Figure 3. Net photoelectric cross section per hydrogen atom as a function of energy (after Morrison and McCammon 1983).

Table 1. Start parameters (Hellier *et al.* 1987) and derived parameters for EX Hya.

Parameter	Starting value	Derived value
$M_{wd}(M_{\odot})$	0.78	0.78
$R_{wd}(10^9 \text{ cm})$	0.65	0.65
$R_1(R_{wd})$	10	10.
$R_2(R_{wd})$	7	7.
$\dot{M}(10^{16} \text{ g s}^{-1})$	1	4
inclination $i$	$78^{\circ}$	$70^{\circ}$
offset angle $\beta$	$10^{\circ}$	$8^{\circ}$
filling factor $f$	1.0	0.7
$f_1$	1.0	$(1 + 3 \cos^2 \theta_1)^3$
$f_2$	0.5	$(\frac{90-\theta_2}{90})^{0.5} + 0.5$

### 3. RESULTS AND DISCUSSION

Figure 4 shows the variation of the column density as a function of interaction radius ( $\Delta R = 0.3$  fixed), interaction zone ( $R_1$  fixed) and the accretion rate.  $\Delta R$  is  $R_1 - R_2$  here. The absorption length at B ( $l$ ) results from the above geometric equation (Eq. 1):

$$l \sim \frac{\sin^2 \theta_1}{\sin^2 \theta} (R_1 - R_2). \quad (7)$$

The column density at B, which is responsible for the modulation of X-rays in the accretion funnel, can now be estimated with  $N_{HI} = \rho \times l$ . As clear in Figure 4a and 4b, the variation of  $R_1$  is not so sensitive to the variation of the column density, and also the modulation in result, although this variation plays an important role in the intensity of the X-ray radiation near the magnetic pole of the compact star. This insensitivity can be argued also for the variation of  $\frac{\Delta R}{R}$  less than 0.3. In this first model approach the parameters  $R_1$  and  $R_2$  are therefore fixed to the literature values as  $10R_{wd}$  and  $7R_{wd}$  respectively.

The total intensity of the radiation emitted toward the observer is constant because at any phase 36 point sources are visible. For the calculation of the observed modulation it is important to estimate the amount of the column density which the emission from source experiences in the line of sight at a given phase. The column densities for given accretion rates are calculated in our accretion geometry at each phase and are plotted in Figure 4c. The comparison of Figure 4c with Figure 3 shows that at low accretion rate can not explain the observed modulation. Our model calculation requires an accretion rate of at least  $3 \times 10^{16} \text{gs}^{-1}$  to reproduce the observational data in contrast to the accretion rate of  $< 10^{16} \text{gs}^{-1}$  estimated until now.

The light curves calculated for different energies (2.2, 4.0, 5.1, 6.2, and 8.1 keV from top to bottom) are shown in Figure 5. This energy dependence is expected from the adapted energy dependent cross section (see Figure 3). Rosen *et al.* (1988) have made a numerical simulation similar to our method. But, their calculation gives no quantitative information about the modulation depth since it has been calculated only for the phases between 0.25 and 0.75 as King and Lasota (1990) criticized. In contrast to our model the radiation of the point sources from the lower pole has not been taken into account by their model.

Some further experiments with this phenomenological model varying another model parameter can be undertaken. One of the interesting results to be mentioned is the model dependence on the structure of the accretion funnel. Figure 6 represents the modulation depth of the X-ray light curve as a function of energy for different filling factors (partial covering). The modulation depth is here defined as

$$\text{Modulation depth (\%)} = \frac{F_{max} - F_{min}}{F_{max}} \times 100, \quad (8)$$

where  $F_{max}$  and  $F_{min}$  are the maximum and minimum flux in the light curve at a given energy.

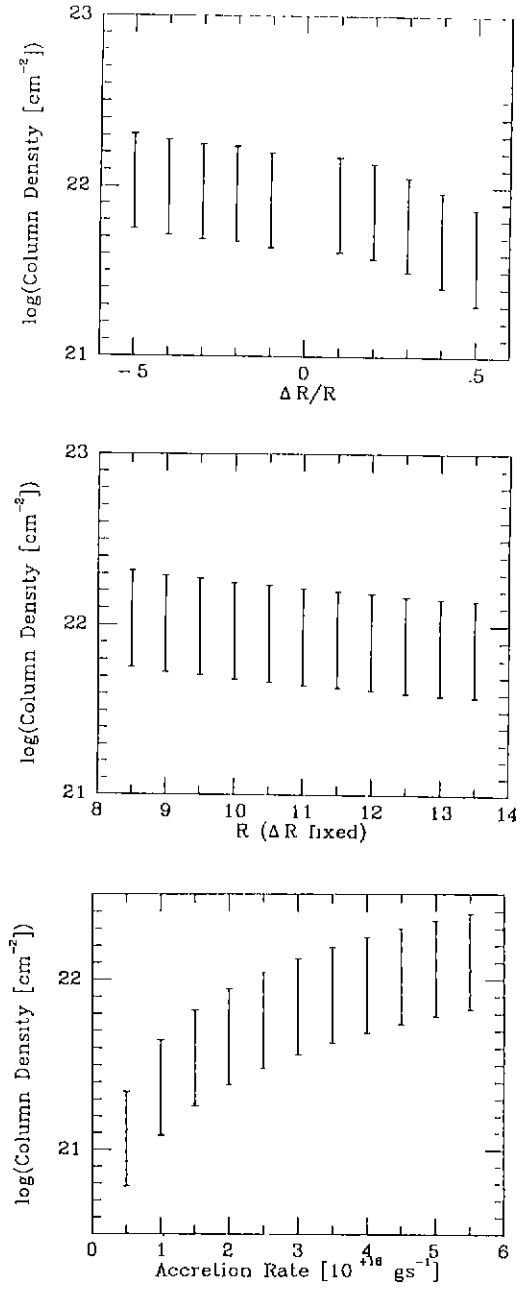


Figure 4. Column density for different model parameters. The vertical bars indicate the range of the column density for the different azimuthal angle (rotational phase).



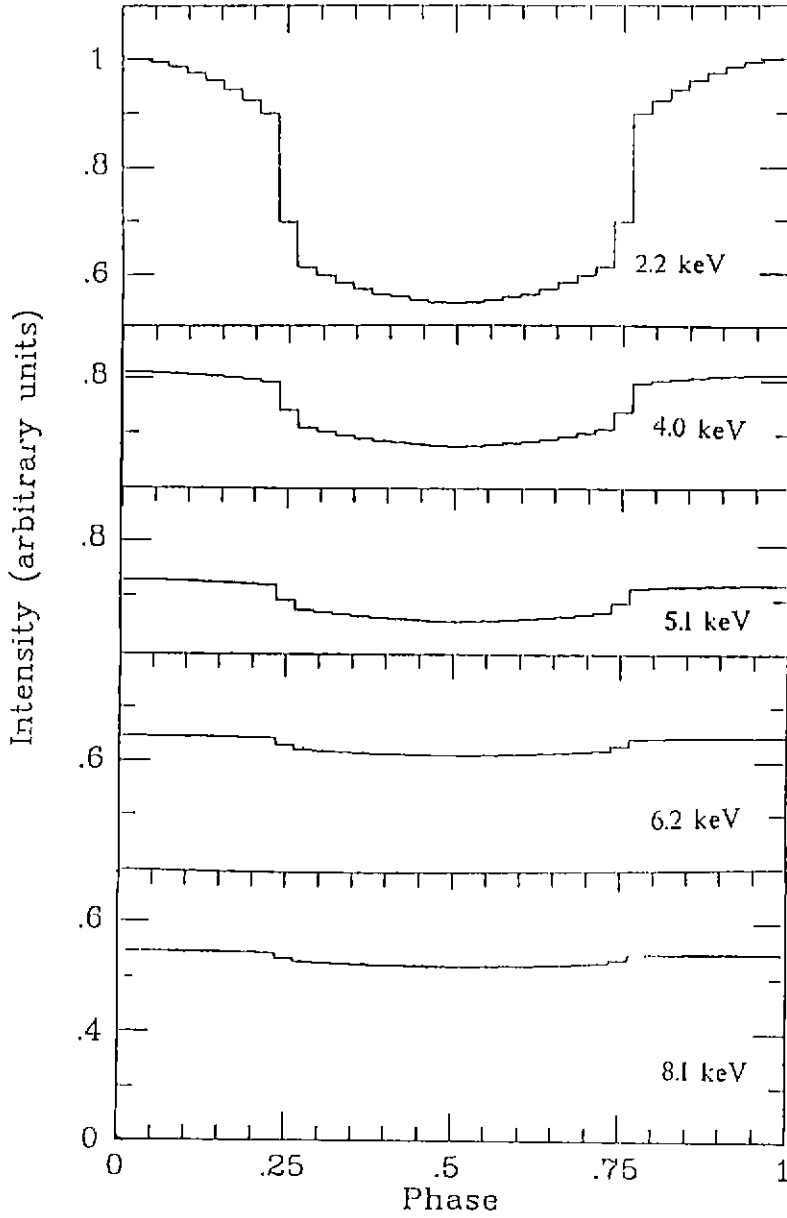


Figure 5. Calculated light curves for the derived parameter at some different energies.

It can be seen that a simple absorber ( $f = 1$ ) can not explain the observed modulation. The matter with small filling factor absorbs less radiation than that with higher filling factor. As a result of it the modulation becomes smaller. This qualitative result is given also by Norton and Watson. The crosses denote the observations of Beuermann and Osborn(1985). Results with another model parameter will be discussed in Kim and Beuermann (1993).

In Figure 7 we compare the results of our calculation with the observational data of Beuermann and Osborn (1985). Observed modulation depths at some energy bands and our calculations are given in Table 2. As can be seen in Figure 7 and Table 2 the derived parameters agree well with the observations as long as the X-ray modulation is concerned. It has, however, to be noted that there could also exist another combination of the parameters giving a better agreement with the observations. But as a first result toward a phenomenological calculation of the material transport from the accretion disc through the magnetosphere our result may be sufficient.

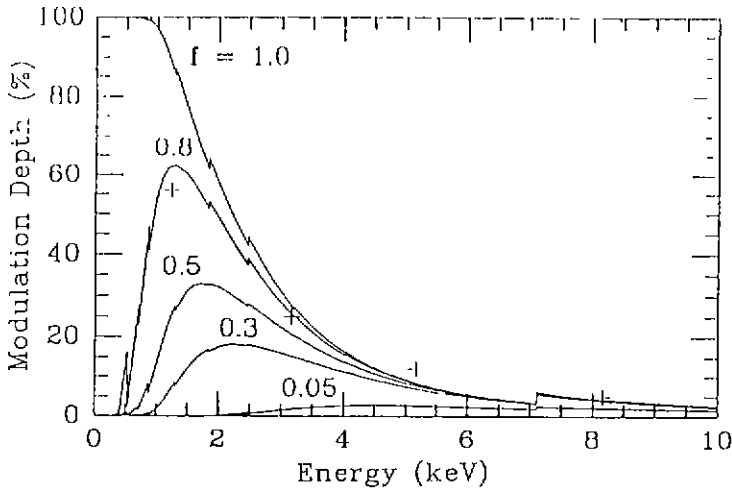


Figure 6. Modulation depth for different filling factors (partial covering). The crosses denote the observed modulation depth (Beuermann and Osborne 1985).

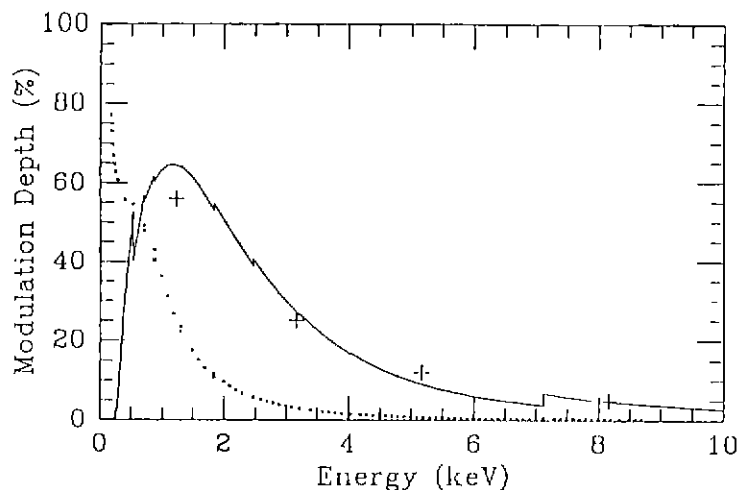


Figure 7. Comparison of results with observational data for EX Hya.  
 pointed curve : modulation depth calculated with start parameter.  
 solid curve : modulation depth calculated with our final parameter.  
 + : observed modulation depth (Beuermann and Osborne 1985).

Table 2. Observed modulation depth (%) and result of our model calculation at different energy bands (keV) for EX Hya.

0.05 - 2.0	2.0 - 4.0	4.0 - 6.0	6.0 - 10.0	reference
$64 \pm 4$	$23 \pm 1$	$15 \pm 2$	$12 \pm 6$	Cordova and Riegler (1979)
$58 \pm 4$	$27 \pm 2$	$14 \pm 4$	$18 \pm 8$	Kruszewski <i>et al.</i> (1981)
$56 \pm 4$	$25 \pm 2$	$12 \pm 3$	$5 \pm 10$	Beuermann and Osborne(1985)
$57 \pm 4$	$28 \pm 2$	$14 \pm 3$	$10 \pm 14$	Cordova <i>et al.</i> (1985)
57.9	31.8	10.8	4.9	this paper

#### 4. CONCLUDING REMARKS AND FURTHER WORK

The above results show that the X-ray modulation with the rotational phase can be explained by photoabsorption along the accretion funnel and self occultation by the compact star. This is the first reasonable phenomenological model calculation of the spin modulated X-ray radiation in intermediate polars. The main uncertainty in our model is caused by the distribution functions ( $f_1$  and  $f_2$ ). Since until now no theoretical work concerning these functions has been done we use, at the moment, our phenomenological function. A theoretical approach must be undertaken in order to understand this mechanism in more detail.

In this simplified approach we have used a cross section for the neutral gas only. This must be modified in more proper model considering that the matter in the funnel may be partially ionized. This is also the first time that the reasonable column densities in the accretion funnel have been adapted. In the previous papers (Imamura and Durison 1983; Norton and Watson 1989, and others) the column density just near the hard X-ray emitting region have been used which is different from the column density in the accretion funnel used in this paper (Figure 1b). This idea must also be justified by application to other IP's in further work.

The absorbed X-rays may heat the matter in the accretion funnel and produce optical light. The optical spectrum due to this reprocessing can be obtained from the energy balance between input and output energy. This approach has been undertaken by Kim (1992) in order to enlarge the capability of our model. Its results will also be presented elsewhere.

#### REFERENCES

- Beuermann, K. & Osborne, J. 1985, *Space Sci. Rev.*, 40, 117.  
 Cordova, F. A., Mason, K. O. & Kahn, S. M. 1985, *MNRAS*, 210, 7.  
 Cordova, F. A. & Riegler, G. R. 1979, *MNRAS*, 188, 103.  
 Hellier, C., Mason, K. O. & Rosen, S. R. 1987, *MNRAS*, 228, 463.  
 Imamura, J. M. & Durison, R. H. 1983, *ApJ*, 268, 291.  
 Kim, Y. 1992, Dissertation, Technische Universität Berlin, Germany.  
 Kim, Y. & Beuermann, K. 1993, AA, in preparation.  
 King, A. R. & Lasota, J. P. 1990, *MNRAS*, 247, 214.  
 Kruszewski, A., Mewe, R., Heise, J., Chlebowski, T. Van Dijk, W. & Bakker, R. 1981, *Space Sci. Rev.*, 30, 221.  
 Morrison, R. & McCammon, D. 1983, *ApJ*, 270, 119.  
 Norton, A. J. & Watson, M. G. 1989, *MNRAS*, 237, 853.  
 Rosen, S. R., Mason, K. O. & Cordova, F. A., 1988, *MNRAS*, 231, 549.